*Psychological Medicine* (2016), **46**, 2549–2560. © Cambridge University Press 2016
doi:10.1017/S0033291716001380

ORIGINAL ARTICLE

# Risperidone-induced topological alterations of anatomical brain network in first-episode drug-naive schizophrenia patients: a longitudinal diffusion tensor imaging study

**M. Hu[1,2], X. Zong[1], J. Zheng[3], J. J. Mann[2], Z. Li[1], S. P. Pantazatos[4], Y. Li[3], Y. Liao[1,5], Y. He[1], J. Zhou[1], D. Sang[6], H. Zhao[6], J. Tang[1,5]*, H. Chen[3]*, L. Lv[7,8]* and X. Chen[1,9,10,11]***

[1] *Mental Health Institute of the Second Xiangya Hospital, Central South University, 139 Middle Renmin Road, Changsha, Hunan 410011, People's Republic of China*
[2] *Division of Molecular Imaging and Neuropathology, New York State Psychiatric Institute and Departments of Psychiatry and Radiology, Columbia University, 1051 Riverside Drive, Box 42, New York, NY 10032, USA*
[3] *Key Laboratory for NeuroInformation of the Ministry of Education, School of Life Science and Technology, University of Electronic Science and Technology of China, Chengdu 610054, People's Republic of China*
[4] *Division of Molecular Imaging and Neuropathology, New York State Psychiatric Institute and Departments of Psychiatry, Columbia University, New York, NY 10032, USA*
[5] *Department of Psychiatry and Biobehavioral Sciences, UCLA Semel Institute for Neuroscience, David Geffen School of Medicine, Los Angeles, CA 90024, USA*
[6] *Department of Radiology, Henan Mental Hospital, the Second Affiliated Hospital of Xinxiang Medical University, Xinxiang, Henan 453002, People's Republic of China*
[7] *Department of Psychiatry, Henan Mental Hospital, the Second Affiliated Hospital of Xinxiang Medical University, Xinxiang, Henan 453002, People's Republic of China*
[8] *Henan Key Laboratory of Biological Psychiatry, Henan Mental Hospital, Xinxiang Medical University, Xinxiang, Henan 453002, People's Republic of China*
[9] *The China National Clinical Research Center for Mental Health Disorders, 139 Middle Renmin Road, Changsha, Hunan 410011, People's Republic of China*
[10] *National Technology Institute of Psychiatry, 139 Middle Renmin Road, Changsha, Hunan 410011, People's Republic of China*
[11] *Key Laboratory of Psychiatry and Mental Health of Hunan Province, 139 Middle Renmin Road, Changsha, Hunan 410011, People's Republic of China*

**Background.** It remains unclear whether the topological deficits of the white matter network documented in cross-sectional studies of chronic schizophrenia patients are due to chronic illness or to other factors such as antipsychotic treatment effects. To answer this question, we evaluated the white matter network in medication-naive first-episode schizophrenia patients (FESP) before and after a course of treatment.

**Method.** We performed a longitudinal diffusion tensor imaging study in 42 drug-naive FESP at baseline and then after 8 weeks of risperidone monotherapy, and compared them with 38 healthy volunteers. Graph theory was utilized to calculate the topological characteristics of brain anatomical network. Patients' clinical state was evaluated using the Positive and Negative Syndrome Scale (PANSS) before and after treatment.

**Results.** Pretreatment, patients had relatively intact overall topological organizations, and deficient nodal topological properties primarily in prefrontal gyrus and limbic system components such as the bilateral anterior and posterior cingulate. Treatment with risperidone normalized topological parameters in the limbic system, and the enhancement positively correlated with the reduction in PANSS-positive symptoms. Prefrontal topological impairments persisted following treatment and negative symptoms did not improve.

**Conclusions.** During the early phase of antipsychotic medication treatment there are region-specific alterations in white matter topological measures. Limbic white matter topological dysfunction improves with positive symptom reduction. Prefrontal deficits and negative symptoms are unresponsive to medication intervention, and prefrontal deficits are potential trait biomarkers and targets for negative symptom treatment development.

*Received 25 November 2015; Revised 11 May 2016; Accepted 12 May 2016; First published online 24 June 2016*

**Key words**: First-episode schizophrenia, longitudinal studies, networks, schizophrenia, topology, white matter.

* Address for correspondence: X. Chen, J. Tang, H. Chen and L. Lv, Mental Health Institute of the Second Xiangya Hospital, Central South University, Changsha, Hunan, People's Republic of China. (Email: chenxghn@gmail.com; tangjinsonghn@gmail.com; chenhf@uestc.edu.cn; lvluxian@126.com)

## Introduction

Over a century ago, it was proposed that schizophrenia is a disorder arising from pathological alterations in the brain's association fibers (Wernicke, 1906), and since then much evidence of white matter abnormalities has emerged from postmortem studies (Stephan *et al.* 2009; Farkas *et al.* 2010). More recently, diffusion tensor imaging (DTI) techniques have provided evidence of white matter pathology in schizophrenia *in vivo* (Ellison-Wright & Bullmore, 2009; Skudlarski *et al.* 2013). Brain regions are connected by a complex white matter network known as the human connectome (Sporns *et al.* 2005). The topological organization of this anatomical network is vital for efficient information segregation and integration among brain regions. The application of graph theory to DTI data permits quantification of both integration and segregation properties of the fiber network (Watts & Strogatz, 1998). Individual differences in topological organizations of white matter networks are substantially hereditable (Bohlken *et al.* 2014). Graph analytical studies have found some consistent topological abnormalities, such as prefrontal topological deficits in unaffected first-degree relatives at high genetic risk for developing schizophrenia (Shi *et al.* 2012; Collin *et al.* 2014), leading us to hypothesize that part of the pattern of structural network topology observed in this disease may mediate the genetic effect as an endophenotype or biological trait. More extensive anatomical network topological deficits were reported in chronic schizophrenia patients (CSP), such as topological impairments in the prefrontal, cingulate and occipital gyri, insula, pallidum and caudate (Van den Heuvel *et al.* 2010, 2013; Zalesky *et al.* 2011; Wang *et al.* 2012; Collin *et al.* 2014). However, these investigations in CSP are difficult to rule out the network topologic abnormalities being a consequence of disease progression or other factors, particularly antipsychotic treatment effects.

To separate chronic stage disease-related findings from those related to treatment and treatment response, longitudinal studies that examine first-episode psychosis before medication is started are needed. Although there is still a lack of follow-up studies directly examining antipsychotic effects on the topological characteristics of white matter networks, three longitudinal studies of first-episode schizophrenia patients (FESP) have reported region-specific antipsychotic medication effects on measures of white matter integrity, such as fractional anisotropy (FA). One study found increased FA in the cingulum and uncinate in FESP after 12 weeks of medication (Reis Marques *et al.* 2014). The two other studies found decreased FA in frontal, occipital and parietal regions after short-term treatment (Wang *et al.* 2013; Szeszko *et al.* 2014). In addition, using functional magnetic resonance imaging (MRI), Achard & Bullmore (2007) found that a single dose of sulpiride (400 mg) appeared to have detrimental effects on topological parameters (network efficiency) of cingulate gyrus and temporal cortex in healthy people; Carbonell *et al.* (2014) demonstrated that dopamine depletion can reduce local efficiency in limbic regions, further supporting a relationship between brain network topology and dopamine signaling. Given this evidence, a reasonable prediction is that antipsychotic medications would have effects on fiber network topological parameters. A longitudinal DTI study to specifically examine how antipsychotic medications influence white matter topology would be a powerful complement to a study of drug-naive FESP.

The current study investigates topological alterations of the anatomical network using baseline MRI scans within 12 months of psychosis onset in FESP who had never been treated with an antipsychotic agent, and a second scan after the baseline scan following treatment with risperidone for 8 weeks. To our knowledge, this is the first longitudinal DTI study to explore the effect of risperidone monotherapy on anatomical graph-theoretic topological properties in a relatively large study sample ($n = 42$) of treatment-naive FESP. We hypothesized that: (*a*) abnormalities would be present in the topological characteristics of the white matter network in medication-naive FESP when compared with healthy volunteers, particularly in the prefrontal cortex, limbic/paralimbic system and subcortical structures based on previous studies (Zalesky *et al.* 2011; Wang *et al.* 2012; Van den Heuvel *et al.* 2013; Collin *et al.* 2014); and (*b*) antipsychotic treatment would influence the topological organizations of the above-mentioned systems in patients, but this effect would be differentially localized based on prior reports (Achard & Bullmore, 2007; Carbonell *et al.* 2014; Reis Marques *et al.* 2014; Szeszko *et al.* 2014). We also conducted an exploratory investigation to examine whether alterations of white matter topological properties would relate to clinical symptom response to medication.

## Method

### *Participants*

A total of 80 right-handed Chinese Han people were recruited, including 42 treatment-naive FESP and 38 age-, gender- and education-matched healthy volunteers. These participants were all in our previous study (Zong *et al.* 2015). All the patients were recruited for this study at Henan Province Mental Health Center, the Second Affiliated Hospital of Xinxiang Medical University, Henan, China. Diagnoses of schizophrenia

https://doi.org/10.1017/S0033291716001380 Published online by Cambridge University Press

were determined with the Structured Clinical Interview for DSM-IV-TR, patient version (SCID-I/P). All the patients had less than 1 year since onset of psychotic symptoms, and mean age was 24.86 (S.D. = 4.80) years (range 18 to 37 years; online Supplementary Table S1). Healthy volunteers were recruited by advertisement and screened using the SCID-NP, non-patient edition for lifetime absence of any psychiatric illness, and did not have a family history of psychiatric illness in any first-degree relative. Any individual with a history of physical illness, neurological disorder, or alcohol or drug abuse was excluded from the study.

All procedures were approved by the ethics committee of the Second Xiangya Hospital and the Second Affiliated Hospital of Xinxiang Medical University. Written informed consent was obtained from all participants, who were permitted to discontinue participation from this research at any time. One patient discontinued during the DTI scan at baseline, and also withdrew from the follow-up MRI scan. Three other patients withdrew from the follow-up MRI scans. Consequently, MRI data were collected from 41 patients at baseline, 38 patients after treatment, and 38 healthy controls. All 42 patients completed clinical assessments.

### *Medication and clinical assessments*

All schizophrenia patients were stabilized on risperidone monotherapy at a dosage of 4–6 mg/day for 8 weeks. Mood stabilizers and antidepressants were not used. The efficacy and safety of risperidone was assessed weekly by clinical interviews. During the 8-week treatment, no serious adverse effects occurred. Symptom severity of all patients was evaluated at baseline and followed up with the 30-item Positive and Negative Syndrome Scale (PANSS) (Kay *et al.* 1987).

### *Acquisition of MRI data*

All patients had high-resolution T1-weighted three-dimensional images and DTI scans both at baseline when they were free from antipsychotics and after the 8-week treatment, while controls were scanned only once. Participants were scanned on a 3 T Siemens MRI scanner (Germany) with a 16-channel head coil. Whole-brain volume sagittal T1-weighted images were obtained with a three-dimensional spoiled gradient echo pulse sequence [repetition time/echo time (TR/TE) = 1900 ms/2.52 ms, flip angle = 9°, field of view (FOV) = 250 × 250, slice thickness = 1.0 mm, gap = 0 mm, number of excitations = 1, 176 slices] (Fig. 1*a*). DTI images were collected using a single-shot spin-echo planar imaging (EPI) with a twice-refocused balanced echo sequence to reduce eddy current distortions (TR/TE = 7500/93 ms, FOV = 240 × 240, acquisition matrix = 128 × 128, flip angle = 90°, $b = 0$ and 1000 s/mm$^2$ along 64 non-collinear directions, slice thickness = 3.0 mm, 45 contiguous axial slices) (Fig. 1*b*). All data processing used the same methods and quality thresholds, and was checked for noise, motion and artifacts. Any individual with movement greater than 1.5 mm translation or more than 1.5° rotation was excluded.

### *Construction of anatomical brain network*

We used the Automated Anatomical Labeling (AAL) atlas as a volumetric template with 90 whole-brain regions (Tzourio-Mazoyer *et al.* 2002). Statistical Parametric Mapping (SPM8; http://www.fil.ion.ucl.ac.uk/spm) was implemented to perform the preprocessing and map the AAL atlas to each individual's subject space. Each individual T1-weighted image was co-registered to the B0 image by a linear transformation in the native diffusion space. Co-registered structural images were mapped to the Montreal Neurological Institute (MNI) T1 template by utilizing an affine transformation and a series of non-linear warps. Using nearest-neighbor interpolation and inverted MNI transformation parameters, the volumetric (AAL) template was warped from MNI space to the native diffusion space, resulting in 90 network nodes (45 in each hemisphere) (Fig. 1*c*).

FSL 4.1(FMRIB's Diffusion Toolbox; http://www.fmrib.ox.ac.uk/fsl) was used to correct head motion and eddy current distortions for DTI. The linear least-squares fitting method was used to estimate diffusion tensor models at each voxel with the Diffusion Toolkit software (TrackVis.org), and the Fiber Assignment by Continuous Tracking (FACT) algorithm was used to perform whole-brain fiber tracking in native diffusion space using TrackVis 0.5.1. The DTI tracking followed procedures as described in a previous study (Zhang *et al.* 2011) (Fig. 1*d*), and path tracing was terminated if the FA was <0.1 or the angle between the current and the previous path segment was greater than 45°. We constructed weighted graphs according to the number of reconstructed streamlines between each pair of regions (Fig. 1*e*). One of the reconstructed brain networks was removed from the control group as its network density was over mean plus three standard deviations of the group. Failure to remove those outliers may lead to false-negative findings (De Reus & van den Heuvel, 2013).

### *Network organization and topological properties*

Graph theoretical analysis was utilized to calculate the topological characteristics of the weighted brain structural network at nodal and overall levels in all participants (Fig. 1*f*). Nodal characteristics consist of: (1) nodal degree ($k_i^W$); (2) clustering coefficiency ($CC_{nodal}$); (3) path length ($PL_{nodal}$); (4) betweenness centrality ($b_i^W$); (5) nodal efficiency ($E_{nodal}$). Overall

https://doi.org/10.1017/S0033291716001380 Published online by Cambridge University Press

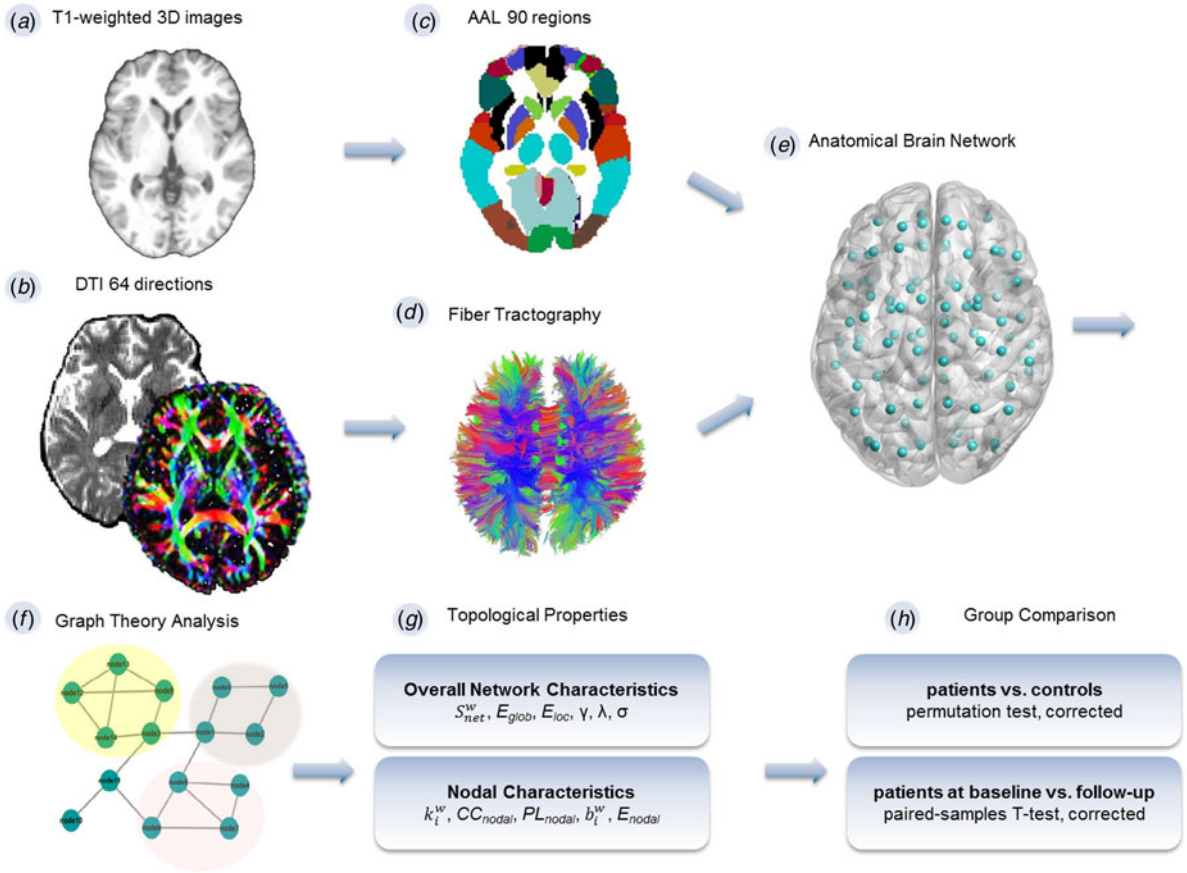


**Fig. 1.** Schematic overview of construction of anatomical network. (*a*) Acquisition of T1-weighted images. (*b*) Diffusion tensor images (DTI). (*c*) Parcellation of whole brain with Automated Anatomical Labeling (AAL) template consisting of 90 unique brain regions. (*d*) Whole-brain fiber tracking. (*e*) Depiction of white matter network. (*f*) Calculation of the topological characteristics with graph theory. (*g*) Computation of both overall and nodal network properties. (*h*) Between-group comparison. The topological characteristics of patients both at baseline and follow-up, respectively, were compared with controls using a permutation test (corrected). Within-individual comparisons were performed using paired-samples *t* tests (corrected). 3D, Three-dimensional; $S^W_{net}$, net strength; $E_{glob}$, global efficiency; $E_{loc}$, local efficiency; $\gamma$, normalized clustering coefficients; $\lambda$, normalized path lengths; $\sigma$, small-worldness; $k^W_i$, nodal degree; $CC_{\text{nodal}}$, clustering coefficiency; $PL_{\text{nodal}}$, path length; $b^W_i$, betweenness centrality; $E_{nodal}$, nodal efficiency.

network characteristics include: (1) net strength ($S^W_{net}$); (2) global efficiency ($E_{glob}$); (3) local efficiency ($E_{loc}$); (4) normalized clustering coefficients ($\gamma$); (5) normalized path lengths ($\lambda$); (6) small-worldness ($\sigma$) (Fig. 1*g*).

The Brain Connectivity Toolbox (http://www.brainconnectivtiy-toolbox.net) was used to calculate the network properties (Rubinov & Sporns, 2010). In brief, $k^W_i$ is equal to the sum of the reconstructed streamlines terminating in a node. $CC_{nodal}$ is defined as the fraction of how close the node's neighbors are to being a clique (complete graph). $PL_{nodal}$ refers to the average of the shortest path from the node to all the other nodes in the network. The $b^W_i$ is equivalent to the number of all shortest paths in the network that pass through a node. Efficiency was defined as the reciprocal or inverse of path length, $E_{glob}$ is the average inverse shortest path length in the network, and $E_{loc}$ is the $E_{glob}$ computed on node neighborhoods (Bullmore & Sporns, 2012). The $S^W_{net}$ is defined as the gross of all neighboring link weights. A set of random networks were created by randomizing the connections of the network, keeping the degree distribution and sequence of the matrix intact (Rubinov & Sporns, 2010). Finally, small-worldness ($\sigma = \gamma/\lambda$) was used to describe complex networks that have a high efficiency and high clustering, respectively, which can be figured by the two attributes, namely normalized clustering coefficients ($\gamma = CC_{\text{real}}/CC_{\text{random}}$), and normalized path lengths ($\lambda = PL_{\text{real}}/PL_{\text{random}}$) (Watts & Strogatz, 1998).

The $E_{glob}$, $PL_{nodal}$ and $\lambda$ properties reflect the integration of the network, while the $E_{loc}$, $CC_{nodal}$ and $\gamma$ reflect the segregation. The architectural features $k^W_i$, $S^W_{net}$ and $\sigma$ represent the network architecture, and the $b^W_i$ represent the measure of centrality.

https://doi.org/10.1017/S0033291716001380 Published online by Cambridge University Press

### *Group differences in topological properties*

The anatomical network topological characteristics of patients at baseline and after the 8-week treatment, respectively, were compared with healthy volunteers using the permutation test. Briefly, for a given characteristic, we firstly computed the group difference between FESP and controls. Then all participants were randomly assigned into two groups, and we recalculated the group difference between the two random groups. This process was repeated for 5000 permutations and a sampled group difference null distribution for every topological property was obtained. We computed the proportion of the actual group difference in the 5000 random group differences. Finally, any between-group difference greater than the 95th percentile of the empirical distribution in a two-tailed test can be declared significant at an $\alpha = 0.05$. Comparisons in patients before and after treatment were performed using paired-samples $t$ tests ($\alpha = 0.05$). As the examined nodal topological measures are dependent, we performed false discovery rate (Storey, 2002) correction in 90 × 3 multiple tests (cut-off value 0.05) for each nodal characteristic. Comparisons of global network characteristics were corrected by the Bonferroni method ($p < 0.05$) (Fig. 1*h*).

### *Statistical analysis*

Statistical analyses were performed with the SPSS 13.0 software package (SPSS Inc., USA). The independent-samples $t$ test or $\chi^2$ test were used to compute the group differences of demographic data. The paired-samples $t$ test was used to compare patients' longitudinal alterations of PANSS scores. Correlations between either baseline network metrics (exhibiting between-group differences) and clinical variables (PANSS scores), or longitudinal alterations (with significance) in anatomical network topological properties and improvement of clinical symptoms (PANSS scores) were computed by multiple linear regression analysis, controlling for age and gender.

## Results

### *Demographics*

A total of 42 patients met the criteria of treatment-naive FESP. Healthy volunteers were well matched with patients on age, gender, years of education, and alcohol and tobacco use ($p$'s > 0.05) (online Supplementary Table S1).

### *Longitudinal alterations of clinical symptoms*

After the 8-week treatment, patients had pronounced reductions in PANSS-total scores, positive scores (PANSS-P) and general psychopathology (PANSS-G), but no significant alterations in negative scores (PANSS-N) (online Supplementary Table S1).

### *Schizophrenia- and treatment-related alterations in nodal characteristics*

At baseline, patients had lower $k_i^W$ ($p = 0.032$, corrected) and $E_{\text{nodal}}$ ($p = 0.040$, corrected) in the right anterior cingulate and paracingulate gyri (ACG) and decreased $k_i^W$ ($p = 0.035$, corrected) in the left ACG compared with controls (Table 1; Fig. 2*a*). There were also reduced $CC_{\text{nodal}}$ in the left ($p = 0.035$, corrected) and right ($p = 0.048$, corrected) posterior cingulate gyrus (PCG) (Table 1; Fig. 2*a*). After 8 weeks of treatment, there was an increase in the $k_i^W$ ($p = 0.023$, corrected) and $E_{\text{nodal}}$ ($p = 0.048$, corrected) of the right ACG, and the $k_i^W$ ($p = 0.043$, corrected) of the left ACG (Table 1; Fig. 3*a*). $CC_{\text{nodal}}$ in the left ($p = 0.042$, corrected) and right ($p = 0.049$, corrected) PCG also increased (Table 1; Fig. 3*a*). Moreover, all the observed nodal parameters bilaterally in the ACG and PCG at the 8-week follow-up did not differ from controls ($p$'s > 0.05, corrected) (Table 1).

Patients had lower baseline $k_i^W$ ($p = 0.019$, corrected) and $E_{nodal}$ ($p = 0.013$, corrected) in the left superior frontal gyrus medial orbital (SFGmedorb), and lower $k_i^W$ ($p = 0.020$, corrected) in the right pallidum compared with controls (Table 1; Fig. 2*a*). After treatment, there were no longitudinal changes in nodal metrics of the left SFGmedorb or right pallidum ($p$'s > 0.05, corrected) (Table 1). Moreover, compared with controls, patients after 8 weeks of treatment continued to exhibit lower $k_i^W$ ($p = 0.019$, corrected) and $E_{nodal}$ ($p = 0.041$, corrected) in the left SFGmedorb, and lower $k_i^W$ ($p = 0.049$, corrected) in the right pallidum (Table 1).

Patients revealed no differences in the left amygdala and left parahippocampal gyrus (PHG) compared with controls at baseline ($p$'s > 0.05, corrected). After the 8-week treatment, however, patients showed increased $k_i^W$ ($p = 0.003$, corrected) and $E_{nodal}$ ($p = 0.005$, corrected) in the left amygdala, and $k_i^W$ ($p = 0.044$, corrected) and $E_{nodal}$ ($p = 0.030$, corrected) in the left PHG (Table 1, Fig. 3*a*).

At baseline patients had no significant difference in $k_i^W$ of the left caudate nucleus (CAU) ($p > 0.05$, corrected) compared with controls. After treatment, the $k_i^W$ ($p = 0.013$, corrected) in the left CAU decreased (Table 1).

See online Supplementary Table S2 for more detail about nodal topographical characteristics. We also normalized these characteristics of each node by dividing the mean value of each metric of random network to control the potential bias, and got similar results as described above (online Supplementary Table S3).

https://doi.org/10.1017/S0033291716001380 Published online by Cambridge University Press

**Table 1.** *Nodal topological characteristics of healthy comparison controls and first-episode schizophrenia patients for baseline and follow-up data*

| | | Patients[b] | | | | |
|---|---|---|---|---|---|---|
| Nodal property | Controls[a] ($n = 37$) | Baseline ($n = 41$) | Week 8 ($n = 38$) | Analysis[c] | Analysis[d] | Analysis[e] |
| Left ACG/AAL31 | | | | | | |
| $k_i^W$ | 1022.0 (836.0) | 671.8 (514.4) | 868.2 (824.1) | 0.035* | 0.043* | 0.066 |
| Right ACG/AAL32 | | | | | | |
| $k_i^W$ | 702.0 (740.0) | 423.6 (453.7) | 555.7 (596.7) | 0.032* | 0.023* | 0.062 |
| $E_{nodal}$ | 45.5 (24.8) | 33.8 (20.7) | 38.3 (23.1) | 0.040* | 0.048* | 0.076 |
| Left PCG/AAL35 | | | | | | |
| $CC_{nodal}$ | 54.9 (24.5) | 43.6 (18.4) | 48.6 (21.7) | 0.035* | 0.042* | 0.056 |
| Right PCG/AAL36 | | | | | | |
| $CC_{nodal}$ | 54.3 (21.4) | 45.1 (17.3) | 49.6 (22.8) | 0.048* | 0.049* | 0.060 |
| Left SFGmedorb/AAL25 | | | | | | |
| $k_i^W$ | 459.9 (332.4) | 245.6 (179.7) | 292.7 (213.7) | 0.019* | 0.052 | 0.019* |
| $E_{nodal}$ | 32.3 (15.1) | 22.1 (10.3) | 24.7 (11.2) | 0.013* | 0.079 | 0.041* |
| Right pallidum/AAL76 | | | | | | |
| $k_i^W$ | 937.9 (555.6) | 721.0 (342.4) | 815.8 (416.4) | 0.020* | 0.060 | 0.049* |
| Left amygdala/AAL41 | | | | | | |
| $k_i^W$ | 150.7 (138.2) | 115.7 (128.1) | 172.7 (128.6) | 0.056 | 0.003* | 0.071 |
| $E_{nodal}$ | 18.1 (10.8) | 15.7 (8.7) | 20.4 (8.5) | 0.071 | 0.005* | 0.055 |
| Left PHG/AAL39 | | | | | | |
| $k_i^W$ | 138.1 (100.6) | 175.4 (153.6) | 182.8 (111.8) | 0.053 | 0.044* | 0.035* |
| $E_{nodal}$ | 16.7 (8.8) | 17.7 (8.6) | 20.2 (9.7) | 0.078 | 0.030* | 0.053 |
| Left CAU/AAL71 | | | | | | |
| $k_i^W$ | 1065.6 (489.3) | 892.6 (427.1) | 769.4 (387.6) | 0.052 | 0.013* | 0.015* |

Values are given as mean (standard deviation).

ACG, Anterior cingulate and paracingulate gyri; AAL, Automated Anatomical Labeling; $k_i^W$, nodal degree; $E_{nodal}$, nodal efficiency; PCG, posterior cingulate gyrus; $CC_{nodal}$, clustering coefficiency; SFGmedorb, superior frontal gyrus medial orbital; PHG, parahippocampal gyrus; CAU, caudate nucleus; DTI, diffusion tensor imaging; MRI, magnetic resonance imaging; FDR, false discovery rate.

[a] One of the reconstructed brain network was removed from the 38 healthy volunteers for its lowest outlier network density.

[b] One of the 42 patients discontinued during the DTI scan at baseline, and also withdrew from the follow-up MRI scan. Three other patients withdrew from the follow-up MRI scans.

[c] Patients at baseline *v.* controls, permutation test with FDR correction.

[d] Patients at baseline *v.* follow-up, paired-samples *t* test with FDR correction.

[e] Patients at follow-up *v.* controls, permutation test with FDR correction.

* Significant difference ($p < 0.05$).

### *Comparisons of overall network characteristics*

Group comparisons showed no significant differences in $\gamma$, $\lambda$, $S_{net}^W$, $E_{glob}$, $E_{loc}$ or $\sigma$ ($p$'s > 0.05, corrected) (online Supplementary Table S4). We provide preliminary evidence that patients' regional topological impairments occur in the context of preserved overall topological organization during the early phase of schizophrenia (see online Supplementary Discussion).

### *Relationships between topological characteristics and clinical variables*

The baseline $CC_{nodal}$ of the left PCG showed a negative correlation with PANSS-G scores ($p = 0.020$, corrected by age and gender, Fig. 2*b*). The post-treatment improvements of $E_{nodal}$ of the right ACG were positively correlated with decreases in PANSS-P scores ($p = 0.048$, corrected by age, gender and baseline $E_{nodal}$ of the right ACG, Fig. 3*b*). However, none of the associations survived Bonferroni correction.

## Discussion

As hypothesized, drug-naive FESP had baseline topological abnormalities of the white matter network, primarily located in limbic system regions such as the bilateral ACG, bilateral PCG, prefrontal area involving the left SFGmedorb, and in the striatum involving the

https://doi.org/10.1017/S0033291716001380 Published online by Cambridge University Press

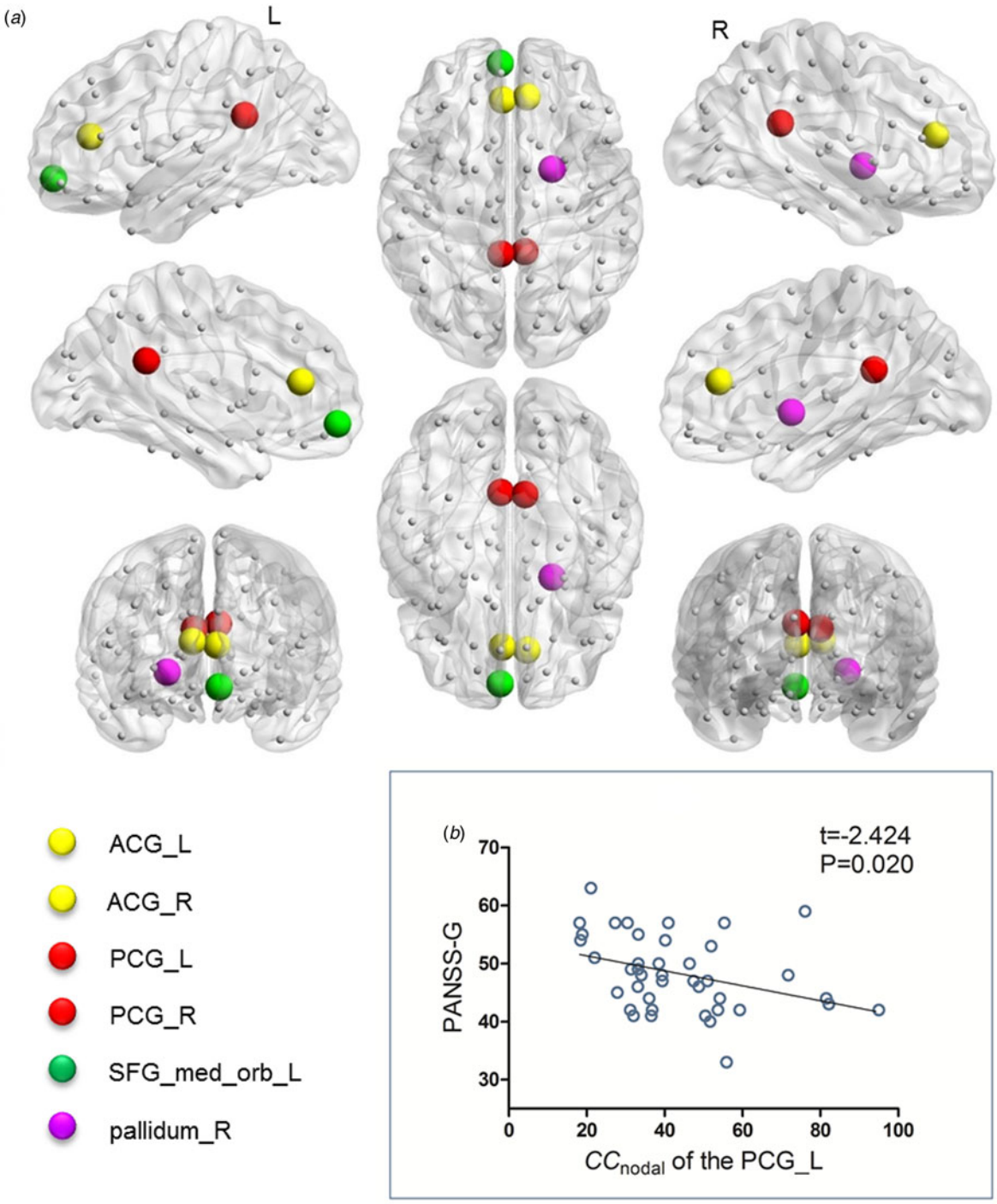


**Fig. 2.** Brain regions showing deficient topological characteristics in anatomical brain networks and the relationship with a clinical variable in drug-naive first-episode schizophrenia patients (FESP). (*a*) Areas of deficient topological attributes in drug-naive FESP relative to healthy controls at baseline. There were significant differences in the bilateral anterior cingulate and paracingulate gyri (ACG), bilateral posterior cingulate gyrus (PCG), left superior frontal gyrus medial orbital (SFG_med_orb_L) and right pallidum (pallidum_R). (*b*) Negative correlation between baseline clustering coefficiency ($CC_{nodal}$) of the left PCG and Positive and Negative Syndrome Scale general psychopathological symptom scores (PANSS-G) in FESP. L, Left; R, right.

right pallidum. These findings suggest that the white matter topological dysfunction of the limbic system, frontal gyrus and striatum may be involved in the pathology of schizophrenia, because they are present early in the course of overt illness and prior to any medication usage. To characterize antipsychotic treatment effects on fiber network topology, participants were rescanned after 8 weeks of risperidone

https://doi.org/10.1017/S0033291716001380 Published online by Cambridge University Press

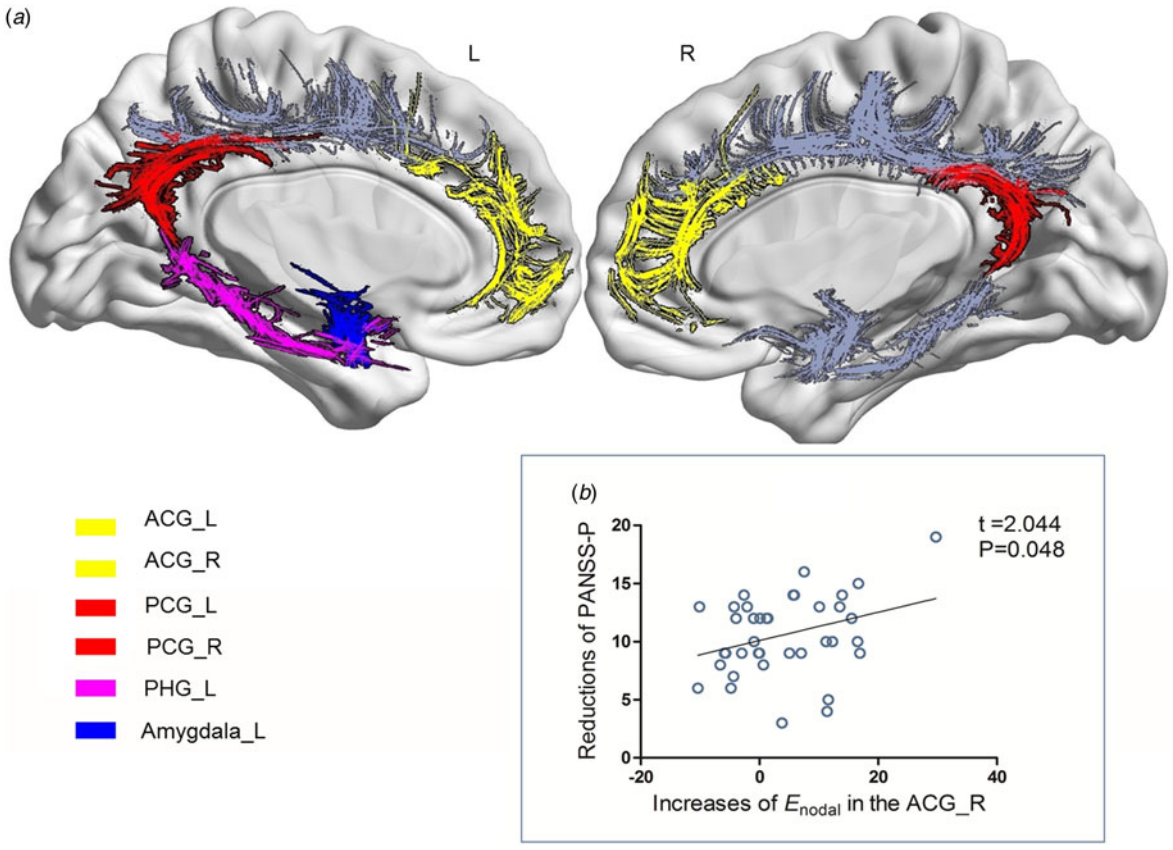


**Fig. 3.** Brain regions showing longitudinal alterations of nodal topological metrics in anatomical brain networks and the relationship with improvement of clinical variable after 8 weeks of risperidone treatment in drug-naive first-episode schizophrenia patients (FESP). (*a*) Areas with alterations of topological attributes in white matter networks after 8 weeks of risperidone treatment of drug-naive FESP. There was improvement of topological properties in the bilateral anterior cingulate and paracingulate gyri (ACG), bilateral posterior cingulate gyrus (PCG), left PHG (PHG-L) and left amygdala (amygdala_L). (*b*) Positive correlation between improvement of nodal efficiency ($E_{\text{nodal}}$) in the right ACG and the reduction in Positive and Negative Syndrome Scale positive symptoms (PANSS-P) score ($p = 0.048$, controlling for age and gender). L, Left; R, right.

monotherapy. The topological disruptions of the limbic system improved in at least one nodal property, while there were no significant changes in the frontal gyrus or right pallidum. Positive symptoms improved and the degree of improvement in the PANSS-P scores correlated with alterations in some indices of topological disruption in the limbic system. However, as these findings did not survive corrections for multiple comparisons, these findings should be considered provisional requiring replication in an independent sample. Antipsychotic therapy failed to normalize either prefrontal topology or improve negative symptoms. Additionally, the topological parameter of the left CAU decreased after antipsychotic medications, and yet did not show any baseline differences when compared with the control group. That may be a medication side effect unrelated to therapeutic benefit or the pathology of schizophrenia or a compensatory effect.

We found baseline deficits in the $k_i^W$ of the bilateral ACG, and $E_{\text{nodal}}$ of the right ACG, suggesting the ACG may have less regional efficiency in transferring information and communication with the rest of its anatomical networks. These 'deficient' topological properties of ACG were improved by 8 weeks of treatment. In addition, patients' reduced baseline $CC_{\text{nodal}}$ of the bilateral PCG showed normalization after treatment, suggesting that risperidone monotherapy may increase the PCG's local efficiency of information transfer. Interestingly, treatment increased topological indices ($k_i^W$ and $E_{nodal}$) in the left PHG and amygdala, while at baseline there were no significant group differences relative to controls, implying a gain-of-efficiency of these two regions in transferring information in the anatomical network. This may reflect a secondary response to the changes of the ACG and PCG, given they are the source of crucial afferent and efferent connections in the limbic system including the PHG and amygdala (Catani *et al.* 2013); or it may be part of the therapeutic effect of the medication or a non-specific side effect. The ACG, PCG, amygdala and PHG are

https://doi.org/10.1017/S0033291716001380 Published online by Cambridge University Press

important components of the limbic system considered to be involved in the physiopathology of schizophrenia (Gur *et al.* 2007; Lahti *et al.* 2009). The limbic damage is regarded as a 'state' marker and actively responds to pharmacological interventions (Lahti *et al.* 2009; Lui *et al.* 2010). Moreover, the cingulate gyrus furnishes the limbic system with the crucial axonal wiring to constitute connectivity to and from other divisions including the amygdala and PHG of the system (Catani *et al.* 2013). White matter abnormalities of these identified regions in schizophrenia have been widely reported in neuroimaging and histopathological studies (Kubicki *et al.* 2003; Farkas *et al.* 2010; Van den Heuvel *et al.* 2010). These implicated nodes included the key cortical (i.e. ACG) and subcortical (i.e. amygdala) structures of the salience network, as well as the posterior component (i.e. PCG) and medial temporal region (including PHG) of the default mode network. Both the salience network and default mode network are proposed to be an important part of the triple network model, a unifying network that is implicated in the cognitive dysfunction and aberrant saliency mapping of schizophrenia and other neuropsychiatric disorders (Menon, 2011). Our current findings of post-treatment increased topological attributes in the PCG, ACG, PHG and amygdala, together with the preliminary evidence suggesting the potential effect of antipsychotic medications on salient (Palaniyappan *et al.* 2012) and default mode network (Sambataro *et al.* 2010), imply that dysfunctions of the triple network are viable therapeutic targets in schizophrenia.

Treatment-related changes of $E_{\text{nodal}}$ in the right ACG positively correlated with reductions in PANSS-P scores after treatment, suggesting that the degree of increase in the right ACG's communication efficiency is linked to improvement in positive symptoms. The ACG plays a role in decision-making, choosing between conflicting options and error detection (Carter *et al.* 2001), and this region's inability in self-monitoring may contribute to the failure to identify one's own inner thoughts from external circumstances, and is therefore a potential neuropathological substrate for positive symptoms (Kubicki *et al.* 2003). The association of abnormalities of the ACG with positive symptoms is in accord with prior studies (Cheung *et al.* 2011; Kates *et al.* 2015). Moreover, salience network dysfunction leads to damaged detection of salient external environment and internal events, with significant self-monitoring consequences (Menon, 2011). Cross-sectional studies suggest a relationship between structural or functional deficits of the ACG within the salience network with psychosis (Palaniyappan *et al.* 2011; Palaniyappan & Liddle, 2012). Our current findings based on a longitudinal design provide further evidence linking post-treatment topological organization alterations of the salience network component and improvement of positive symptoms in schizophrenia. Additionally, we also observed a relationship between baseline $CC_{\text{nodal}}$ of the left PCG and PANSS-G, although, to our knowledge, this is the first study linking PCG topological attributes with severity of general psychopathological symptoms in schizophrenia. Pathology of the PCG has been postulated to cause emotional and cognitive impairments (Maddock, 1999) and thus might underlie the genesis of the general psychopathological symptoms in schizophrenia.

We observed lower $k_i^W$ and $E_{\text{nodal}}$ in the left SFGmedorb at baseline, indicating the possibility of the frontal gyrus's inefficient communication with other brain regions and low regional efficiency in transferring information in the white matter network. The frontal gyrus is strongly implicated in the physiopathology of schizophrenia (Wang *et al.* 2013; Piantadosi & Floresco, 2014). This study provides new support for the frontal dysfunction hypothesis of schizophrenia because our findings are in drug-naive FESP. No improvement of frontal deficits is consistent with other studies (Snitz *et al.* 2005; Van Veelen *et al.* 2011) and suggests that the frontal dysfunction may represent a 'trait' marker of schizophrenia because it responds poorly to antipsychotics. It remains to be seen whether these topological deficits improve when effective treatments for negative clinical symptoms of schizophrenia are identified.

Behavioral outcome and white matter topological changes after treatment initiation can be further understood in the context of the schizophrenia dopamine (DA) hypothesis and risperidone's D2 antagonism (Meyer & Feldon, 2009). More specifically, DA in the mesocortical system (projecting to the prefrontal areas) may be hypoactive and its deficits are proposed to underlie negative symptoms, whereas the mesolimbic DA pathway may be hyperactive and its hyperactivity may be critically involved in the emergence of positive symptoms. Risperidone's antagonism of DA, especially D2 receptors in the limbic areas, is beneficial for positive symptoms. However, risperidone's block effect in the frontal gyrus has no beneficial and perhaps detrimental influence on negative symptoms because patients already have low frontal DA levels. Our observations of no benefit for negative symptoms and no improvement in frontal topological parameters suggest a relationship between frontal topologies and negative symptom severity at baseline.

### *Limitations*

Although structural network graph theory properties appear to have moderate test–retest reliability (Cheng *et al.* 2012), the lack of repeated scans for the control group is a limitation of this study as we cannot exclude

https://doi.org/10.1017/S0033291716001380 Published online by Cambridge University Press

the possibility that the observed topological changes after treatment might be related to test–retest variability. The identified relationship between nodal topologies and clinical symptoms should be considered as exploratory in nature as results did not survive corrections for multiple comparisons.

## Conclusion

In summary, this is the first follow-up DTI study in drug-naive recent onset psychotic patients which demonstrates that topological deficits of anatomical networks may be due to medication effects. Limbic white matter topological dysfunction improves with positive symptom reduction, whereas prefrontal topological deficits appear to be unresponsive to psychopharmacological intervention and may be potential trait biomarkers and targets for negative symptom treatment development. Future studies with more effective treatments for negative symptoms are needed to evaluate their effects on prefrontal topological deficits and to determine whether such deficits may serve as treatment biomarkers.

## Supplementary material

The supplementary material for this article can be found at http://dx.doi.org/10.1017/S0033291716001380

## Acknowledgements

This work was supported by grants from the National Natural Science Foundation of China (81271484 and 81471361 to X.C.; 61533006 to H.C.; 30900486 and 81371480 to J.T.), the National Key Basic Research and Development Program (973) (2012CB517904 to X. C.), the National Institutes of Health (K01MH108721 to S.P.P.), the 863 project (2015AA020505 to H.C.) and the China Scholarship Council Program (to M.H.).

## Declaration of Interest

J.J.M. received royalties for commercial use of the Columbia Suicide Severity Rating Scale (C-SSRS) from the Research Foundation for Mental Hygiene.

## References

**Achard S, Bullmore E** (2007). Efficiency and cost of economical brain functional networks. *PLoS Computational Biology* **3**, e17.

**Bohlken MM, Mandl RC, Brouwer RM, van den Heuvel MP, Hedman AM, Kahn RS, Hulshoff Pol HE** (2014). Heritability of structural brain network topology: a DTI study of 156 twins. *Human Brain Mapping* **35**, 5295–5305.

**Bullmore E, Sporns O** (2012). The economy of brain network organization. *Nature Reviews. Neuroscience* **13**, 336–349.

**Carbonell F, Nagano-Saito A, Leyton M, Cisek P, Benkelfat C, He Y, Dagher A** (2014). Dopamine precursor depletion impairs structure and efficiency of resting state brain functional networks. *Neuropharmacology* **84**, 90–100.

**Carter CS, MacDonald 3rd AW, Ross LL, Stenger VA** (2001). Anterior cingulate cortex activity and impaired self-monitoring of performance in patients with schizophrenia: an event-related fMRI study. *American Journal of Psychiatry* **158**, 1423–1428.

**Catani M, Dell'Acqua F, Thiebaut de Schotten M** (2013). A revised limbic system model for memory, emotion and behaviour. *Neuroscience and Biobehavioral Reviews* **37**, 1724–1737.

**Cheng H, Wang Y, Sheng J, Kronenberger WG, Mathews VP, Hummer TA, Saykin AJ** (2012). Characteristics and variability of structural networks derived from diffusion tensor imaging. *NeuroImage* **61**, 1153–1164.

**Cheung V, Chiu CP, Law CW, Cheung C, Hui CL, Chan KK, Sham PC, Deng MY, Tai KS, Khong PL, McAlonan GM, Chua SE, Chen E** (2011). Positive symptoms and white matter microstructure in never-medicated first episode schizophrenia. *Psychological Medicine* **41**, 1709–1719.

**Collin G, Kahn RS, de Reus MA, Cahn W, van den Heuvel MP** (2014). Impaired rich club connectivity in unaffected siblings of schizophrenia patients. *Schizophrenia Bulletin* **40**, 438–448.

**De Reus MA, van den Heuvel MP** (2013). Estimating false positives and negatives in brain networks. *NeuroImage* **70**, 402–409.

**Ellison-Wright I, Bullmore E** (2009). Meta-analysis of diffusion tensor imaging studies in schizophrenia. *Schizophrenia Research* **108**, 3–10.

**Farkas N, Lendeckel U, Dobrowolny H, Funke S, Steiner J, Keilhoff G, Schmitt A, Bogerts B, Bernstein HG** (2010). Reduced density of ADAM 12-immunoreactive oligodendrocytes in the anterior cingulate white matter of patients with schizophrenia. *World Journal of Biological Psychiatry: the Official Journal of the World Federation of Societies of Biological Psychiatry* **11**, 556–566.

**Gur RE, Loughead J, Kohler CG, Elliott MA, Lesko K, Ruparel K, Wolf DH, Bilker WB, Gur RC** (2007). Limbic activation associated with misidentification of fearful faces and flat affect in schizophrenia. *Archives of General Psychiatry* **64**, 1356–1366.

**Kates WR, Olszewski AK, Gnirke MH, Kikinis Z, Nelson J, Antshel KM, Fremont W, Radoeva PD, Middleton FA, Shenton ME, Coman IL** (2015). White matter microstructural abnormalities of the cingulum bundle in youths with 22q11.2 deletion syndrome: associations with medication, neuropsychological function, and prodromal symptoms of psychosis. *Schizophrenia Research* **161**, 76–84.

**Kay SR, Fiszbein A, Opler LA** (1987). The Positive and Negative Syndrome Scale (PANSS) for schizophrenia. *Schizophrenia Bulletin* **13**, 261–276.

**Kubicki M, Westin CF, Nestor PG, Wible CG, Frumin M, Maier SE, Kikinis R, Jolesz FA, McCarley RW, Shenton ME** (2003). Cingulate fasciculus integrity disruption in

schizophrenia: a magnetic resonance diffusion tensor imaging study. *Biological Psychiatry* **54**, 1171–1180.

**Lahti AC, Weiler MA, Holcomb HH, Tamminga CA, Cropsey KL** (2009). Modulation of limbic circuitry predicts treatment response to antipsychotic medication: a functional imaging study in schizophrenia. *Neuropsychopharmacology: Official Publication of the American College of Neuropsychopharmacology* **34**, 2675–2690.

**Lui S, Li T, Deng W, Jiang L, Wu Q, Tang H, Yue Q, Huang X, Chan RC, Collier DA, Meda SA, Pearlson G, Mechelli A, Sweeney JA, Gong Q** (2010). Short-term effects of antipsychotic treatment on cerebral function in drug-naive first-episode schizophrenia revealed by "resting state" functional magnetic resonance imaging. *Archives of General Psychiatry* **67**, 783–792.

**Maddock RJ** (1999). The retrosplenial cortex and emotion: new insights from functional neuroimaging of the human brain. *Trends in Neurosciences* **22**, 310–316.

**Menon V** (2011). Large-scale brain networks and psychopathology: a unifying triple network model. *Trends in Cognitive Sciences* **15**, 483–506.

**Meyer U, Feldon J** (2009). Neural basis of psychosis-related behaviour in the infection model of schizophrenia. *Behavioural Brain Research* **204**, 322–334.

**Palaniyappan L, Liddle PF** (2012). Does the salience network play a cardinal role in psychosis? An emerging hypothesis of insular dysfunction. *Journal of Psychiatry and Neuroscience: JPN* **37**, 17–27.

**Palaniyappan L, Mallikarjun P, Joseph V, White TP, Liddle PF** (2011). Reality distortion is related to the structure of the salience network in schizophrenia. *Psychological Medicine* **41**, 1701–1708.

**Palaniyappan L, White TP, Liddle PF** (2012). The concept of salience network dysfunction in schizophrenia: from neuroimaging observations to therapeutic opportunities. *Current Topics in Medicinal Chemistry* **12**, 2324–2338.

**Piantadosi PT, Floresco SB** (2014). Prefrontal cortical GABA transmission modulates discrimination and latent inhibition of conditioned fear: relevance for schizophrenia. *Neuropsychopharmacology: Official Publication of the American College of Neuropsychopharmacology* **39**, 2473–2484.

**Reis Marques T, Taylor H, Chaddock C, Dell'Acqua F, Handley R, Reinders AA, Mondelli V, Bonaccorso S, Diforti M, Simmons A, David AS, Murray RM, Pariante CM, Kapur S, Dazzan P** (2014). White matter integrity as a predictor of response to treatment in first episode psychosis. *Brain: a Journal of Neurology* **137**, 172–182.

**Rubinov M, Sporns O** (2010). Complex network measures of brain connectivity: uses and interpretations. *NeuroImage* **52**, 1059–1069.

**Sambataro F, Blasi G, Fazio L, Caforio G, Taurisano P, Romano R, Di Giorgio A, Gelao B, Lo Bianco L, Papazacharias A, Popolizio T, Nardini M, Bertolino A** (2010). Treatment with olanzapine is associated with modulation of the default mode network in patients with schizophrenia. *Neuropsychopharmacology: Official Publication of the American College of Neuropsychopharmacology* **35**, 904–912.

**Shi F, Yap PT, Gao W, Lin W, Gilmore JH, Shen D** (2012). Altered structural connectivity in neonates at genetic risk for schizophrenia: a combined study using morphological and white matter networks. *NeuroImage* **62**, 1622–1633.

**Skudlarski P, Schretlen DJ, Thaker GK, Stevens MC, Keshavan MS, Sweeney JA, Tamminga CA, Clementz BA, O'Neil K, Pearlson GD** (2013). Diffusion tensor imaging white matter endophenotypes in patients with schizophrenia or psychotic bipolar disorder and their relatives. *American Journal of Psychiatry* **170**, 886–898.

**Snitz BE, MacDonald 3rd A, Cohen JD, Cho RY, Becker T, Carter CS** (2005). Lateral and medial hypofrontality in first-episode schizophrenia: functional activity in a medication-naive state and effects of short-term atypical antipsychotic treatment. *American Journal of Psychiatry* **162**, 2322–2329.

**Sporns O, Tononi G, Kotter R** (2005). The human connectome: a structural description of the human brain. *PLoS Computational Biology* **1**, e42.

**Stephan KE, Friston KJ, Frith CD** (2009). Dysconnection in schizophrenia: from abnormal synaptic plasticity to failures of self-monitoring. *Schizophrenia Bulletin* **35**, 509–527.

**Storey JD** (2002). A direct approach to false discovery rates. *Journal of the Royal Statistical Society: Series B* (*Statistical Methodology*) **64**, 479–498.

**Szeszko PR, Robinson DG, Ikuta T, Peters BD, Gallego JA, Kane J, Malhotra AK** (2014). White matter changes associated with antipsychotic treatment in first-episode psychosis. *Neuropsychopharmacology: Official Publication of the American College of Neuropsychopharmacology* **39**, 1324–1331.

**Tzourio-Mazoyer N, Landeau B, Papathanassiou D, Crivello F, Etard O, Delcroix N, Mazoyer B, Joliot M** (2002). Automated anatomical labeling of activations in SPM using a macroscopic anatomical parcellation of the MNI MRI single-subject brain. *NeuroImage* **15**, 273–289.

**Van den Heuvel MP, Mandl RC, Stam CJ, Kahn RS, Hulshoff Pol HE** (2010). Aberrant frontal and temporal complex network structure in schizophrenia: a graph theoretical analysis. *Journal of Neuroscience: the Official Journal of the Society for Neuroscience* **30**, 15915–15926.

**Van den Heuvel MP, Sporns O, Collin G, Scheewe T, Mandl RC, Cahn W, Goni J, Hulshoff Pol HE, Kahn RS** (2013). Abnormal rich club organization and functional brain dynamics in schizophrenia. *JAMA Psychiatry* **70**, 783–792.

**Van Veelen NM, Vink M, Ramsey NF, van Buuren M, Hoogendam JM, Kahn RS** (2011). Prefrontal lobe dysfunction predicts treatment response in medication-naive first-episode schizophrenia. *Schizophrenia Research* **129**, 156–162.

**Wang Q, Cheung C, Deng W, Li M, Huang C, Ma X, Wang Y, Jiang L, Sham PC, Collier DA, Gong Q, Chua SE, McAlonan GM, Li T** (2013). White-matter microstructure in previously drug-naive patients with schizophrenia after 6 weeks of treatment. *Psychological Medicine* **43**, 2301–2309.

**Wang Q, Su TP, Zhou Y, Chou KH, Chen IY, Jiang T, Lin CP** (2012). Anatomical insights into disrupted small-world networks in schizophrenia. *NeuroImage* **59**, 1085–1093.

**Watts DJ, Strogatz SH** (1998). Collective dynamics of 'small-world' networks. *Nature* **393**, 440–442.

**Wernicke C** (1906). *Grundrisse der Psychiatrie (Plans of Psychiatry)*. Thieme: Leipzig, Germany.

**Zalesky A, Fornito A, Seal ML, Cocchi L, Westin CF, Bullmore ET, Egan GF, Pantelis C** (2011). Disrupted axonal fiber connectivity in schizophrenia. *Biological Psychiatry* **69**, 80–89.

**Zhang Z, Liao W, Chen H, Mantini D, Ding J-R, Xu Q, Wang Z, Yuan C, Chen G, Jiao Q** (2011). Altered functional–structural coupling of large-scale brain networks in idiopathic generalized epilepsy. *Brain* **134**, 2912–2928.

**Zong X, Hu M, Li Z, Cao H, He Y, Liao Y, Zhou J, Sang D, Zhao H, Tang J, Lv L, Chen X** (2015). *N*-acetylaspartate reduction in the medial prefrontal cortex following 8 weeks of risperidone treatment in first-episode drug-naive schizophrenia patients. *Scientific Reports* **5**, 9109.